PHILOSOPHICAL TRANSACTIONS OF THE ROYAL SOCIETY A MATHEMATICAL, PHYSICAL & ENGINEERING SCIENCES

Static solitary waves as limits of discretization: a plausible argument

G. Domokos

Phil. Trans. R. Soc. Lond. A 1997 **355**, 2099-2116
doi: 10.1098/rsta.1997.0112

Static solitary waves as limits of discretization: a plausible argument

By Gábor Domokos

Department of Strength of Materials, Technical University of Budapest, H-1521 Budapest, Hungary

We investigate special limits of the classical Euler buckling problem, arguing that the solution-family 'imitating' (without mass forces) the propagation of a dynamic solitary wave cannot be obtained as a limit from Euler's problem, only from its discretized version. Although we can not prove this claim rigorously, we prove other related statements that make the conjecture strongly plausible. Our results yield access to some open questions related to the discretized problem; also they show some new aspects of spatially chaotic behaviour.

1. Introduction

In this paper we will investigate special limits of the classical planar Euler buckling, a boundary value problem (BVP) describing the behaviour of an elastic beam under axial static force, discussed by Euler (1744) (cf. Love 1927). It is well-known that the homoclinic solution of the corresponding initial value problem (IVP) provides a spatially localized configuration (loop) that also solves the *dynamical* equation of the elastic line and proves to be a solitary wave. The dynamics of flexible rods, yielding solitary waves as solutions, is studied in detail by Coleman & Dill (1992), Maddocks & Dichmann (1994) provide a variational characterization. Naturally, Euler's BVP is not capable of describing the propagation of this wave. In one possible BVP interpretation (for alternative see § 2) the homoclinic solution corresponds to infinite force (instead of infinite length, as in the IVP) and the loop, shrinking to infinitesimal size, is located exactly at the middle of the beam (at least for the first mode solution). However, there exists a family $\mathcal{W}$ of BVP solutions, corresponding to the arbitrary location of the infinitesimal loop, 'imitating' the propagation of the dynamical wave. In this case the dynamics evolves amongst the set $\mathcal{W}$ of non-isolated static shapes, generated by a continuous shift transformation. The only member of $\mathcal{W}$ that can be obtained as a limit from Euler's problem is the homoclinic solution itself. The paper presents the conjecture, supported by a plausible argument, that all of $\mathcal{W}$ can be reached as a limit of the *discretized* BVP.

The fact that the continuous BVP does not converge to $\mathcal{W}$, pointing out the degenerate character of this BVP, is not very surprising. As demonstrated by Domokos & Holmes (1993*b*), there exist arbitrarily small smooth perturbations of the bending stiffness that result in drastic changes in the global bifurcation diagram, including the appearance of arbitrarily high numbers of 'parasitic' solutions. These solutions were already noticed in discrete analogues of nonlinear BVPs more than 15 years ago, (cf. Bohl 1979; Beyn 1982; Peitgen & Schmitt 1981). Peitgen *et al.* (1981) call

Phil. Trans. R. Soc. Lond. A (1997) **355**, 2099–2116
Printed in Great Britain

these solutions 'numerically irrelevant' (NIS). It is true that from the point of view of numerical computations they merely present an embarrassment, however, Domokos & Holmes (1993*a*) showed that parasitic solutions can be important and relevant in mechanical systems, and not only in discrete ones (Domokos & Holmes 1993*b*). This idea is carried further in this study: by using some results of Bohl (1979) and Peitgen *et al.* (1981) we investigate the relationship between limits corresponding to parasitic solutions and show the direct mechanical meaning of these limits.

The degeneracy (or structural instability) of the Euler BVP is a result of a high degree of symmetry. By perturbing the BVP one can obtain more generic cases, which, in turn, might prove to be vastly more complex than the original, classical problem. A special perturbation is discretization, either in the sense of discretizing the ordinary differential equation (ODE) by a step-by-step integrator, or, in the sense of discretizing the mechanical problem to a sequence of equal rigid links, coupled by linear torsional springs. The investigation of Domokos & Holmes (1993*a*) showed that the two discretizations can be made equivalent, moreover, the resulting map is none other than the *standard map*. Domokos & Holmes (1993*a*) investigated the extremely rich structure of the discrete BVP, proving the existence of parasitic solutions (not present in the continuous model) and characterizing them.

In this paper this study will be pursued further with the specific goal of explaining the solution family $\mathcal{W}$ as a limit. The key idea is that in contrast to the continuous BVP which possesses one parameter (the force), the discrete one has a second one: the number of links. With suitable adjustment of these two parameters one can obtain *several different* limits, two of which, $\mathcal{H}$ and $\mathcal{C}$, will be explicitly demonstrated. Moreover, we will prove that $\mathcal{H} \subset \mathcal{W} \subset C$, suggesting in a plausible way that $\mathcal{W}$ itself is a special limit of the discrete BVP.

Besides supporting this argument, the tools and results of the paper help to answer a long-standing question: as already reported by Gáspár & Domokos (1989), the discrete BVP exhibits different behaviour for *odd* and *even* numbers of links. Apparently the investigation of the limits provides the key to this question.

After reviewing earlier results and stating the problem in § 2 we proceed to the new material. In § 3 we introduce special limit sets (not discussed earlier) and formulate our conjecture about wave-like solutions. The discrete problem is scrutinized in § 4, leading to observations supporting the conjecture. Finally, in § 5 we use these observations to introduce the labelling of branches and to explain the odd–even paradox. We also point out the relationship to Markov processes and draw conclusions.

This paper is aimed towards engineers, the arguments appeal to mechanical intuition and are not rigorous in the strict analytical sense. We do not claim mathematical originality for the 'observations', however. We believe that they are relevant from the engineering point of view. Whenever possible we will refer to mathematical results and discuss their connection to the investigated specific mechanical problem. The emphasis is on the mechanical interpretation of non-trivial mathematical concepts, such as chaotic and random behaviour, convergence to degenerate limits. We hope that this mechanical illustration can contribute to deeper understanding.

2. Euler buckling and its limit set $\mathcal{H}$

We recall the classical planar Euler buckling problem (cf. Euler 1744; Love 1927), corresponding to a simply supported slender linearly elastic rod of length L with uniform cross section and bending stiffness EI (E denoting Young's modulus and I

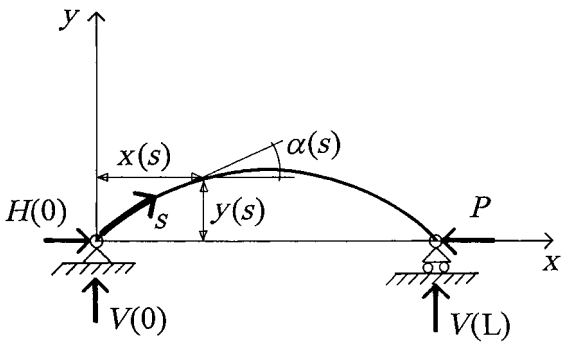

Figure 1. Euler's buckling problem

denoting the moment of inertia of the cross section), infinite axial and shear stiffness, loaded by an axial force P. Euler (1744) provided an essentially complete analysis of this classical problem, which we summarize below. As is customary, we model the (deformed) shape by a plane curve $(x(s), y(s))$ parametrized by the arc length $s \in [0, L]$ (figure 1).

If the load line passes through the supports then there always exist solutions for which the vertical reaction forces vanish identically, although the degenerate case $x(L) = 0$ (discussed by Maddocks (1984)) admits others. We will return to this special case in § 5. By restricting ourselves temporarily to the former non-degenerate solutions ($V(0) = V(L) = 0$), the equilibrium equations may be reduced to the single second order ODE in the slope $\alpha = \arctan(\mathrm{d}y/\mathrm{d}x)$:

$$\alpha'' + \lambda \sin \alpha = 0, \tag{2.1}$$

where $()'$ denotes $(\mathrm{d}/\mathrm{d}s)$ and $\lambda = (P/EI)$. The appropriate boundary conditions, for non-zero load λ, are zero moments

$$\alpha'(0) = 0 = \alpha'(L). \tag{2.2}$$

As Kirchhoff (1859) pointed out, the elastica equilibrium problem is analogous to the pendulum equation (replace $\lambda = P/EI$ by g/l in (2.1)); in fact the three-dimensional elastica is analogous to the more general heavy rigid body (top) problem in dynamics (cf. Love 1927; Mielke & Holmes 1988), of which the pendulum is a special case. This analogy suggests that results for the dynamic initial value problem can be applied to the static boundary value problem and vice versa: a strategy which has been used in studying continuous models (cf. Mielke & Holmes 1988; Thompson & Virgin 1988; ElNaschie 1990). We remark that the $\lambda \to \infty$ limit is equivalent to the $L \to \infty$ limit in the BVP. The latter one is less natural from the engineer's point of view (in a physical experiment λ is more easily varied than L), however, mathematically the two limits coincide. The $L \to \infty$ limit is adopted by Beyn (1990). This limit can be obtained by rescaling the arclength s by $S = as$ and letting $a \to \infty$. By introducing the new variable S into (2.1) and using $(\mathrm{d}\alpha/\mathrm{d}S) = (\mathrm{d}\alpha/\mathrm{d}s)(\mathrm{d}s/\mathrm{d}S) = (\alpha'/a)$; $(\mathrm{d}^2\alpha/\mathrm{d}S^2) = (\alpha''/a^2)$, one arrives at $\alpha''/a^2 + \lambda \sin \alpha = 0$, which, in turn, is equivalent to the $\lambda \to \infty$ limit. The latter will be investigated below.

Equations (2.1) and (2.2) can be solved exactly using Jacobian elliptic functions. For each fixed load $P > n^2\pi^2 EI/L^2$, in addition to the trivial solution $\alpha = 0$, there are n pairs of buckled states containing $1, 2, \ldots, n$ half waves, respectively, which may be uniquely characterized by the angles $\alpha(0) = \pm\alpha_1(P), \pm\alpha_2(P), \ldots, \pm\alpha_n(P)$ with $0 < \alpha_n < \cdots < \alpha_2 < \alpha_1 < \pi$. This statement is perhaps more easily understood

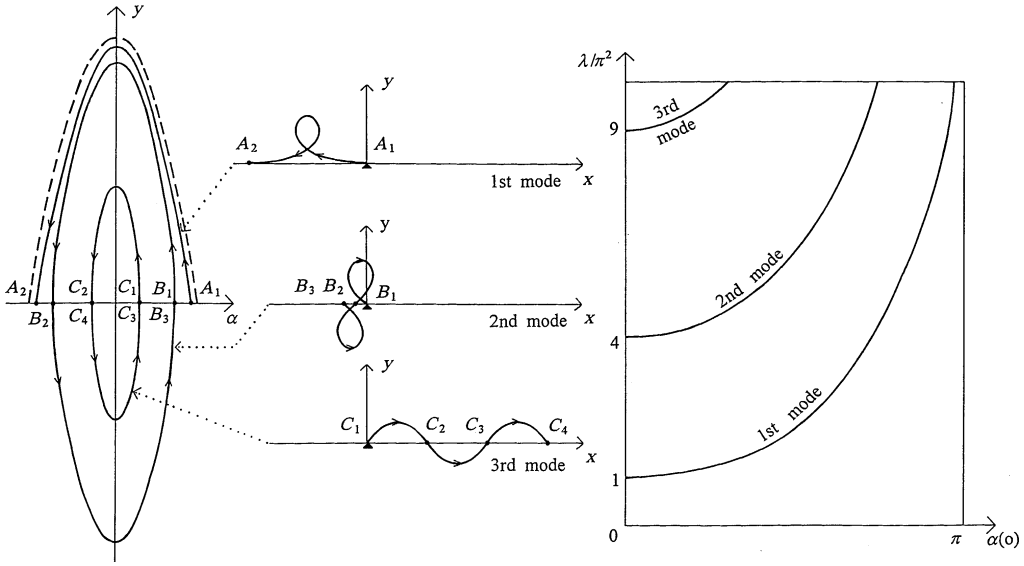

Figure 2. The solutions of the BVP in the physical and phase space and on the global bifurcation diagram.

via the phase portrait of the associated first order system, obtained by introducing the auxiliary variable $y = -\alpha'/\lambda$

$$\begin{aligned} \alpha' &= -\lambda y, \\ y' &= \sin\alpha. \end{aligned} \tag{2.3}$$

This system is Hamiltonian and possesses the first integral

$$-\tfrac{1}{2}\lambda y^2 + \cos\alpha = \cos\alpha(0) = \text{const.} \tag{2.4}$$

The level sets of (2.4) are nested periodic orbits of (2.3) whose period T increases monotonically from $2\pi/\sqrt{\lambda}$ to infinity as $\alpha(0)$ varies from 0 to π. (In fact $T = (4/\sqrt{\lambda})K(\sin(\frac{1}{2}\alpha(0)))$, where K is the complete elliptic integral of the first kind: recall that $K(0) = \frac{1}{2}\pi$ and $K(k) \approx \frac{1}{2}\ln(16/1-k^2)$ as $k \to 1$.) Solutions to the boundary value problem (2.1)–(2.2) are arcs of length L contained in those level sets having periods which are divisors of $2L$. From the monotonicity of T it is clear that these $2n+1$ orbits, including the trivial one, are the only solutions to the BVP. This fact, although with different tools, was already demonstrated by Euler. Figure 2 demonstrates three buckled shapes with the corresponding arcs in the phase plane and the global bifurcation diagram for $\alpha(0) > 0$.

The *homoclinic* solution (dashed line), connecting the two hyperbolic fixed points, is reached in the BVP as $\lambda \to \infty$. As intuitively expected, one can show by manipulating complete and incomplete elliptic integrals that $x(L) \to -L$ as $\lambda \to \infty$. (The limited length of this paper prohibits the demonstration of these calculations, however, they do not support any new claim.) Thus the n loops of the nth buckling mode each shrink to infinitesimal size, the beam becomes 'straight' in the everted limit state. Simultaneously, in the nth mode, as $\lambda \to \infty$, $\alpha'(iL/2n) \to \infty$, $(i = 1, 3, \ldots, 2n-1)$, resulting in n discontinuities of magnitude 2π in $\alpha(s)$. Consequently, the homoclinic solution can be regarded as a discrete family H_n of non-continuous solutions, the nth member H_n of the family being the $\lambda \to \infty$ limit of the nth buckled mode of

the continuous problem

$$H_n(s) = k_n(s)\pi, \quad s \in [0, L], \tag{2.5}$$

where

$$k_n(s) = \begin{cases} -1, & \text{if } 1 < [(2ns/L) \bmod 4] \leqslant 3, \\ 1, & \text{otherwise.} \end{cases} \tag{2.6}$$

We remark that the functions k_n are very similar to the Walsh series w_n introduced by Walsh (1923). In fact, for $n = 2^i$ $(i = 0, 1, \ldots)$ $k_n(s) = w_n(s/L)$. The functions H_n form the homoclinic solution set $\mathcal{H} = \{H_n\}$ $(n = 1, 2, \ldots)$.

3. The solution sets $\mathcal{C}$ and $\mathcal{W}$

Let us now turn back to equations (2.1) and (2.2). Substituting $EI = 0$ (equivalent to $\lambda = \infty$) yields for $P > 0$ the trigonometric equation

$$P \sin \alpha(s) = 0, \tag{3.1}$$

to which the solution set $\mathcal{C}$ belongs

$$\mathcal{C} = \{k(s)\pi\}, \tag{3.2}$$

where

$$k(s) \in \{0, \pm 1, \pm 2, \ldots\}, \quad s \in [0, L]. \tag{3.3}$$

In plain English, the elements of $\mathcal{C}$ are $\alpha(s)$ functions that can have an arbitrary number of discontinuities in $\alpha(s)$, at arbitrary locations, the only restriction being that, away from discontinuities, $\alpha(s)$ remains an integer multiple of π. This huge set, of cardinality greater than the continuum (its cardinal number is $\aleph_2$, as Fraenkel (1923) demonstrates (p. 47, p. 86), cf. also § 5 *c*) contains many interesting subsets. One of them is the already discussed homoclinic solution set $\mathcal{H} \subset \mathcal{C}$; another interesting one-parameter subset $\mathcal{W}_1 \subset \mathcal{C}$ is given by (3.2) and

$$k(s) = \begin{cases} 1, & \text{if } 0 \leqslant s \leqslant s_0, \\ -1, & \text{if } s_0 < s \leqslant L. \end{cases} \tag{3.4}$$

The solution set $\mathcal{W}_1$ could be regarded as the quasi-static image of a single propagating solitary wave since the elements of $\mathcal{W}_1$ represent the (infinitesimal) homoclinic loop at arbitrary locations. Similar sets $\mathcal{W}_n$ (with n parameters) can be constructed in a similar manner as straightforward generalizations of the functions H_n, for the representation of n alternating, simultaneous loops at arbitrary locations. The union of the solution sets $\mathcal{W}_n$ will be denoted by $\mathcal{W}$.

The interest in the set $\mathcal{W}$ is not purely academic. Imperfect subsets of $\mathcal{W}_1$ can be observed in a physical experiment, as we stretch an elastic wire, enforcing a loop. Although this configuration is not stable in the plane (cf. Maddocks 1984), it can be stabilized by the contact force. One can observe that the location of the loop is not uniquely determined; as long as it is sufficiently small compared to the length of the wire, it can be moved back and forth in a range around the midpoint, without violating the boundary conditions. The same phenomenon can be observed in numerical experiments: here the continuous beam is replaced by a sequence of N rigid links coupled by linear springs (for details see the next section). In this model, instead of having a unique loop fixed at the middle, large numbers of adjacent

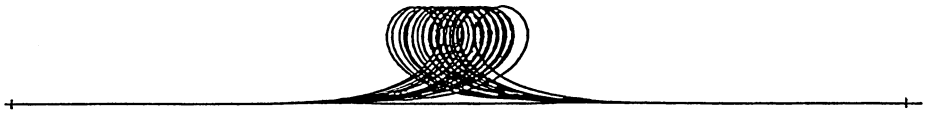

Figure 3. Imperfect subset of $\mathcal{W}_1$ emerging in a numerical experiment ($P = 493.48$, $N = 120$ elements, 59 solutions).

similar solutions appear, which also satisfy the boundary conditions. An example is illustrated in figure 3.

As we can observe, the solutions in $\mathcal{W}$ are physically and numerically relevant. The illustrated numerical example presents a version of $\mathcal{W}_1$ that is imperfect in the sense that both λ and N are finite (but large) instead of infinite, as in the perfect case. These imperfections are manifested in three ways:

(i) instead of a continuum of solution it contains only a finite number;

(ii) the distance between neighbouring solutions is finite instead of infinitesimal; and

(iii) the shape of the solutions is not identical (only very similar) and not identical with the homoclinic loop, either.

We remark that the asymmetry of the illustrated shapes is also a consequence of the imperfection: λ is finite.

It is natural to conjecture that these imperfections can be reduced as the parameter λ and the number N of links increases, thus, in the limit $\mathcal{W}_1$ can be obtained. This prompts the formulation of

Conjecture 3.1. *There exist two functions $\lambda(t)$ and $N(t)$ describing the discretized model with solution set $\mathcal{D}(\lambda, N)$, such that $t \to \infty$ implies $\lambda, N \to \infty$ and $\mathcal{D}(\lambda, N) \to \mathcal{W}$.*

In the next section we will not prove exactly this claim, however, we will show that the larger set $\mathcal{C}$ ($\mathcal{W} \subset \mathcal{C}$) and the smaller set $\mathcal{H}$ ($\mathcal{H} \subset \mathcal{W}$) can both be obtained as special limits of $\mathcal{D}$: in this way we make our conjecture plausible (Polya 1968).

4. The limit sets of the discrete model

In the first part of this section we will define and describe the discrete model, reviewing briefly parts of Domokos & Holmes (1983), to which we refer for more details. The discrete model can be defined either as a discretization of the ODE (2.3), or as a mechanical discretization of the beam, resulting in a sequence of rigid links coupled by linear torsional springs. In the former case a simplectic integrator is preferable (cf. Marsden *et al.* 1991), defining the area preserving map

$$\alpha_{i+1} = \alpha_i - \lambda l y_{i+1}, \quad y_{i+1} = y_i + l \sin \alpha_i. \tag{4.1}$$

Besides being perhaps the simplest such recursive algorithm for numerical solution of the initial value problem associated with (2.3), (4.1) also proves to be the equilibrium condition for the *mechanical* discretization (see figure 4). Each of the N rigid links are of length $l = L/N$, the torsional springs have stiffness EI/l at each joint. Solutions of (4.1) satisfying the discrete boundary conditions

$$y_0 = 0 = y_N, \tag{4.2}$$

not only provide approximations to the exact solutions of the continuum BVP (2.1)–(2.2), but are themselves exact solutions of the discrete mechanical problem with N links.

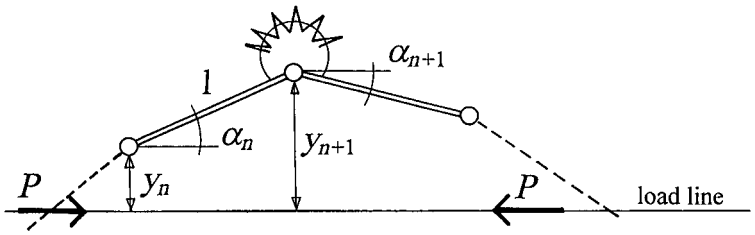

Figure 4. The mechanical interpretation of the discretization.

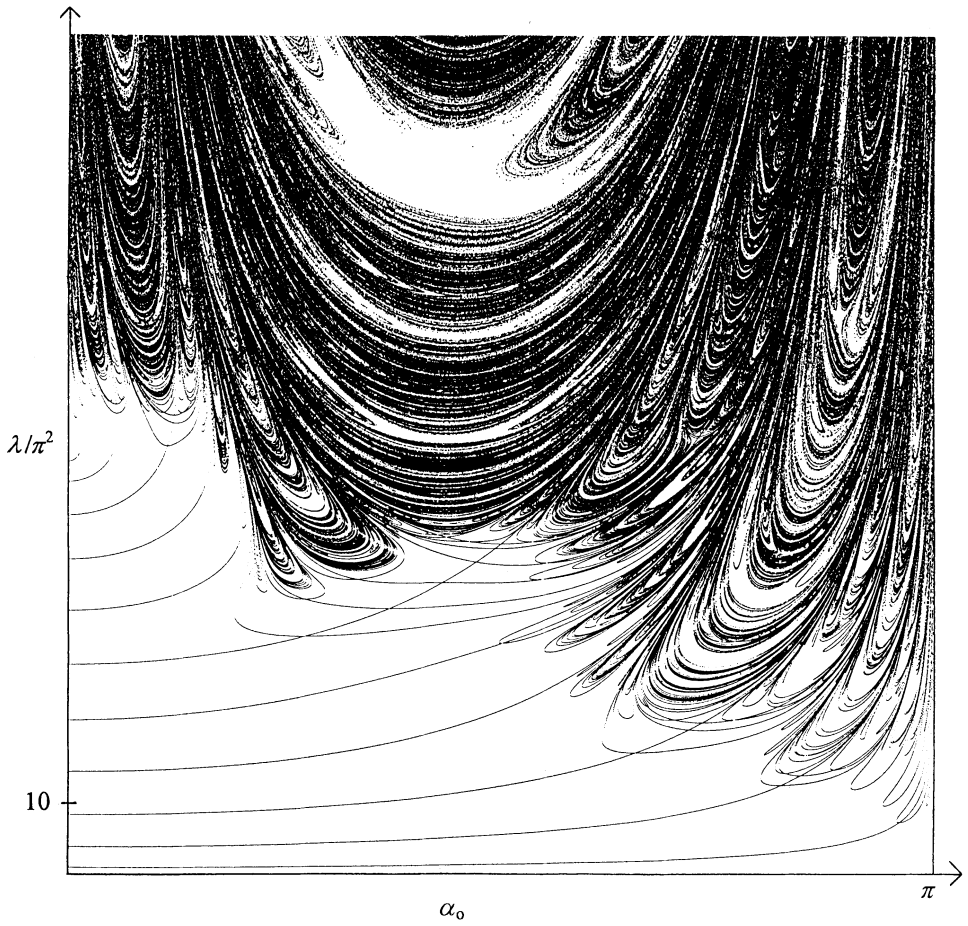

Figure 5. Bifurcation diagram of the discrete model for $N = 12$.

Equation (4.1) can be turned by a simple linear transformation into the *standard map* which has been extensively studied as being perhaps the simplest two-dimensional map providing chaotic solutions. The bifurcation diagrams for the discrete model (4.1)–(4.2) display a radically different structure from that of the continuous problem (2.2)–(2.3). As an example we present the $N = 12$ case in figure 5.

As it is apparent from the figure, besides the primary buckled modes (corresponding to the modes of the continuous model), a large number of other solutions appear in the discrete problem which we call *parasites*. It is a natural question to ask from

where these parasites originate, how can they be organized, and, as perhaps most relevant to our present subject, where do they converge as $\lambda \to \infty$.

The origin of the parasites was already clarified by Bohl (1979). Domokos & Holmes (1993*a*) showed the mechanical relevance of parasites by using properties of the standard map. In addition, we characterized asymptotic behaviour for large λ, but only for the primary branches. Finally, we showed that as λ increases, the number of parasitic solutions in each mode grows beyond any finite number.

The discrete BVP (4.1)–(4.2) has two parameters, λ and N, so the solution set can be written as $\mathcal{D}(\lambda, N)$. Fixing $\lambda = \lambda_0$ and letting $N \to \infty$ is equivalent to applying an integrator with decreasing stepsize: standard ODE theory guarantees the convergence to the continuous BVP (2.2)–(2.3). After reaching that limit one can let $\lambda_0 \to \infty$. As we saw in the previous section, the continuous model converges to the homoclinic solutions. This consideration can be summarized for later reference as follows.

Observation 4.1. $\lim_{\lambda\to\infty}\{\lim_{N\to\infty}[\mathcal{D}(\lambda, N)]\} = \mathcal{H}$.

If we interchange the two limits, the result is more surprising. We can formulate the following.

Observation 4.2. $\lim_{N\to\infty}\{\lim_{\lambda\to\infty}[\mathcal{D}(\lambda, N)]\} = \mathcal{C}$.

As a first step, we deal only with the $\lambda \to \infty$ limit at constant N. This limit is also interesting from the physical point of view: it will inform us on the asymptotic behaviour of the bifurcation diagrams like the one illustrated in figure 5. The solution set $\mathcal{C}_N$ corresponding to this limit is the discrete version of $\mathcal{C}$ and is defined as

$$\mathcal{C}_N = \{k_i\pi\}, \tag{4.3}$$

where

$$k_i \in \{0, \pm1, \pm2, \ldots\}, \quad i \in \{0, 1, \ldots, N-1\}. \tag{4.4}$$

Our (reduced) claim is formulated as follows.

Observation 4.3. $\lim_{\lambda\to\infty}[\mathcal{D}(\lambda, N)] = \mathcal{C}_N$.

The mechanical content of this observation is confirmed by engineering intuition: as we pull with increasing force at the endpoints of the linkage, the slope of each individual member decreases, and in the limit the links are collinear with the line of action of the acting force. The individual solutions contain springs that went through an unspecified number of $k\pi$ rotations. Visualizing this limit is also helpful in understanding the origin of parasites: at a slight release from the infinite load the springs start an unwinding process, leading to the abundant solution structure illustrated in figure 5. Observation 4.3 is not new from the mathematical point of view, the $\lambda \to \infty$ limit of the discretized BVP was investigated by Bohl (1979) and Peitgen *et al.* (1981). The fact that each (unbounded) branch of the BVP converges to an element of $\mathcal{C}_N$ is proven in remark 2.4 of the latter work. The converse, i.e. that to each function in $\mathcal{C}_N$ one branch converges, is demonstrated by Bohl (1979) (cf. also Peitgen *et al.* (1981), corollary 2.5). We remark that these results could be obtained directly by an application of the implicit function theorem to (4.1), rewritten as a three-point discretization of (2.1).

In order to support observation 4.2 one further step is required: the $N \to \infty$ limit of $\mathcal{C}_N$ is a purely geometric construction: by letting $N \to \infty$ the point set defined by

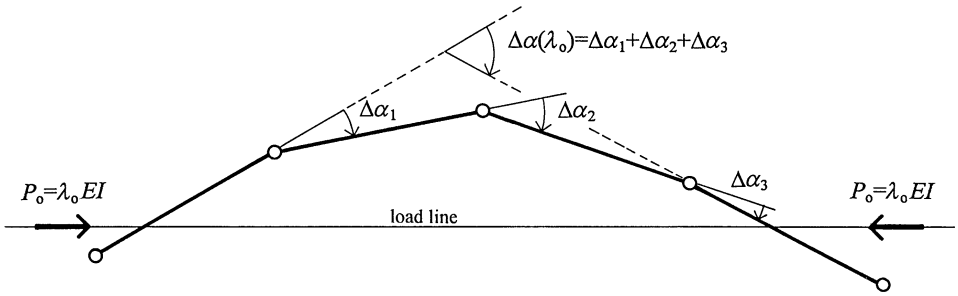

Figure 6. Segment between points on load line.

the discrete model becomes dense in the continuum, in this sense $\lim_{N\to\infty} \mathcal{C}_N = \mathcal{C}$ (cf. § 5 *c*).

The preceding considerations were rather simple, on the other hand, they rely on deeper mathematical results. We are led to the conclusion the sets $\mathcal{H}$ and $\mathcal{C}$ can both be obtained as special limits from the discretized BVP. The former is the set of homoclinic solutions to which the continuous model converges; the latter is a larger set, obtained by substituting $\lambda = \infty$ explicitly into the continuous model. The set $\mathcal{W}$, containing the quasi-static version of solitary wave propagation, is contained in $\mathcal{C}$; meanwhile it contains $\mathcal{H}$ as a subset: $\mathcal{H} \subset \mathcal{W} \subset \mathcal{C}$. These facts support, in a plausible way, conjecture 3.1, stating that $\mathcal{W}$ itself can be constructed as a limit of $\mathcal{D}(\lambda, N)$. (For more details see § 5 *c*.)

(*a*) *Additional mechanical arguments and generalization*

As mentioned before, the claim of observation 4.3 is supported by mathematical results. Nevertheless, we will provide an additional mechanical argument. This reasoning not only provides a better intuitive insight, it also yields access to mechanically more relevant generalizations which cannot be obtained from the cited mathematical results. The generalization to non-uniform discretizations will be used in § 5 *d*.

Observation 4.3 can be decomposed into two statements which we will prove subsequently.

(1) *Each branch of the discrete BVP (4.1)–(4.2) either terminates at finite* λ*, or converges to an element of* $\mathcal{C}_N$*, defined in (4.3)–(4.4).*

The idea of the mechanical proof is to decompose the discrete BVP into a series of segments, starting and ending where the structure intersects the load line (these points need not coincide with the joints). We will show for each of these segments that a finite upper bound valid for all relative angles exists, and via this upper bound the convergence to an element of $\mathcal{C}_N$ can be shown.

We regard a segment between two intersections with the load line, so y_i do not change sign along the segment (without loss of generality, we will assume $y_i \geqslant 0$) and let $\lambda = \lambda_0 < \infty$ (see figure 6).

According to (4.1), relative angles $\Delta\alpha_i = \alpha_i - \alpha_{i-1}$ at any intermediate hinge do not change sign along the segment, either. The total relative angle $\Delta\alpha(\lambda_0)$, measured between the two end-links of the segment can be computed as the sum of all intermediate relative angles. As we move along the branch, neither of the end-links can rotate by more than π, otherwise it would become collinear with the load line and the solution would become the trivial one. (Domokos & Holmes (1993*a*) prove that there are only $N-1$ bifurcations from the trivial solution, corresponding to the primary branches. Consequently, none of the branches can *return* to the trivial

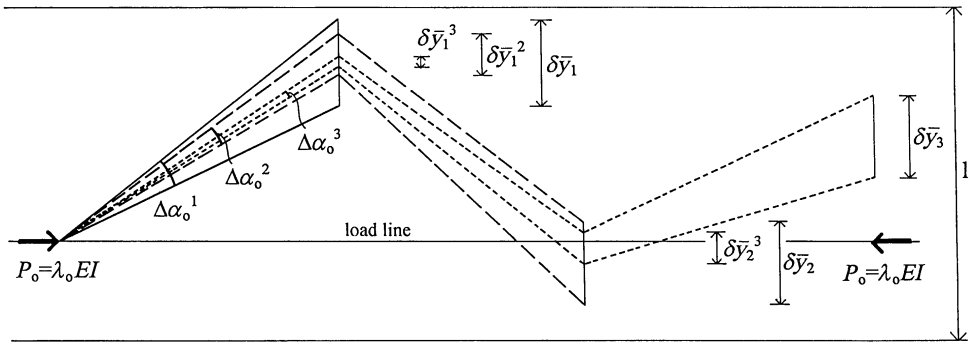

Figure 7. The strip of width l containing the intervals $\delta\bar{y}_i$.

solution.) The limited rotation at the end means that $\Delta\alpha$ is bounded from above: $\Delta\alpha \leqslant \Delta\alpha(\lambda_0) + 2\pi$. This implies the same finite upper bound for all $\Delta\alpha_i$, since we have $\Delta\alpha_i < \Delta\alpha$. As $\lambda \to \infty$, this upper bound enforces via (4.1) $y_i \to 0$, $\sin\alpha_i \to 0$, and, consequently $\alpha_i \to k_i\pi$. Since the structure can be always decomposed into a sequence of such segments, we have proved our claim for all $i \in \{0, 1, \ldots, N-1\}$. (We remark that as λ increases, the length of the investigated segment might change since joints might pass through the load line. However, as they do so, the moment (and thus the relative angle) vanishes; consequently the new link belonging to the segment inherits its absolute angle from the previous one smoothly and thus our considerations are not affected.)

After proving that each branch (not terminated at finite λ) converges to an element of $\mathcal{C}_N$ we proceed to the next part of observation 4.3:

(2) *For any given function in $\mathcal{C}_N$ (defined in (4.3)–(4.4), there exists at least one branch of the BVP (4.1)–(4.2) that converges to the given function.*

According to (4.3)–(4.4), a function contained in the discrete limit set $\mathcal{C}_N$ is defined by a sequence of integers $k_i; i \in \{0, 1, \ldots, N-1\}$, from which the new sequence $\bar{k}_i = k_{i+1} - k_i; i \in \{0, 1, \ldots, (N-2)\}$ can be obtained. Let

$$k_{\max} = \begin{cases} \max\{\bar{k}_i\}, & \text{if } \max\{\bar{k}_i\} > 0, \\ 0, & \text{otherwise,} \end{cases} \tag{4.5}$$

and

$$k_{\min} = \begin{cases} \min\{\bar{k}_i\}, & \text{if } \min\{\bar{k}_i\} < 0, \\ 0, & \text{otherwise.} \end{cases} \tag{4.6}$$

We choose

$$\lambda_0 = \pi(k_{\max} - k_{\min} + 2)/l^2 \tag{4.7}$$

(recall that $l = L/N$) and define a sequence of intervals

$$\delta\bar{y}_i = [\pi(\bar{k}_i - 1)/(l\lambda_0), \quad \pi(\bar{k}_i + 1)/(l\lambda_0)]. \tag{4.8}$$

Our choice (4.7) of λ_0 ensures that all intervals lie within a strip of width l (see figure 7), containing the load line.

Now we will show that there exists a solution of (4.1)–(4.2) such that for every i, $y_i \in \delta\bar{y}_i$ and this solution converges to the prescribed limit function $\alpha_i = k_i\pi$. We construct the solution at $\lambda = \lambda_0$ by induction. Let α_0 go through a complete period: y_1 will cover the interval $[-l, l]$ twice, also it will move through $\delta\bar{y}_1$ twice. From the

corresponding two intervals of α_0 we pick the one that is closer to the prescribed πk_0, let us denote this interval by $\Delta\alpha_0^1$. In the next step we let y_i travel through $\delta\bar{y}_1$: the second link will describe a complete circle, y_2 will move through $\delta\bar{y}_2$ twice. From the corresponding sub-intervals of $\delta\bar{y}_1$ we pick the one (denoted by $\delta\bar{y}_1^2$)that fixes α_1 closer to the prescribed πk_1. As we varied y_1 inside $\delta\bar{y}_1$, α_0 moved within $\Delta\alpha_0^1$. Since $\delta\bar{y}_1^2 \subset \delta\bar{y}_1$, the corresponding interval $\Delta\alpha_0^2 \subset \Delta\alpha_0^1$. As we proceed further, we obtain a nested sequence of intervals $\Delta\alpha_0^i \subset \Delta\alpha_0^{i-1}$ for α_0 and $\delta\bar{y}_j^i \subset \delta\bar{y}_j^{i-1}$ for each y_i, finally the value $y_N = 0$ is fixed by the boundary condition (4.2) and thus it specifies a single point inside the last (smallest) interval. After constructing this solution for $\lambda = \lambda_0$, we let $\lambda_0 \to \infty$. The width d of the strip can be expressed by using (4.7) $d = \pi(k_{\max} - k_{\min} + 2)/(l\lambda_0)$, and as $\lambda_0 \to \infty$, $d \to 0$ and the same holds for all $\delta\bar{y}_i$ intervals, so, finally $y_i \to 0$ and $\alpha_i \to k_i\pi$. Thus we demonstrated one branch that converges to a prescribed function in $\mathcal{C}_N$.

This mechanical argument supports observation 4.3. Now we will show that it can be readily generalized for more generic mechanical systems.

The choice of non-uniform mesh (unequal length l_i for the links) does not change the argument for statement (1). In the argument for (2) we have to consider that the stiffness c_i of the ith spring can be derived as $c_i = 2EI/(l_i + l_{i+1})$, l_i and l_{i+1} denoting the length of the adjacent links. We have to choose the spring with maximal (resp. minimal) *moment*. (The uniform mesh produced equal stiffnesses $c_i = EI/l$, so maximal moment coincided with maximal relative rotation.) Accordingly, in equations (4.5)–(4.6) and (4.8) the sequence $\bar{k}_i$ has to be replaced by $\bar{k}_i c_i$, in (4.7) l has to be replaced by $l_{\min} = \min\{l_i\}$; otherwise the argument is not affected by the choice of non-uniform discretization. This means that the same simple limit is obtained for *all* discretizations.

Physical nonlinearity of the springs can be considered in a similar manner: the sequence $\bar{k}_i$ has to be replaced by $\bar{m}_i(\bar{k}_i)$, where m_i is an *a priori* given function, denoting the moment in the ith spring as a function of the relative angle. The resulting limit behaviour is the same as in the case of linear material behaviour, as long as the functions m_i are strictly monotonic and the first derivative remains finite.

5. Related issues, discussion and conclusions

(*a*) *Branch labels*

The argument for statement (2) actually shows more than the original statement, which claimed that there exists *at least* one branch converging to a given function in $\mathcal{C}_N$. According to the argument this branch is uniquely defined; thus the map defined by our argument has a mutual one-to-one correspondence between branches going to infinity and the functions in $\mathcal{C}_N$. The latter ones are completely described by the integer string $C_N = \{k_i\}$, $i \in \{1, 2, \ldots, N\}$, which could be used to identify all infinite branches uniquely. In previous statements we excluded branches that terminate at finite λ (either at saddle-node or pitchfork critical points). However, numerical evidence indicates that *no such branches exist*. Although we do not formulate an explicit conjecture, we remark that the unique C_N labels probably apply to all branches.

From the mathematical point of view, $\mathcal{C}_N$ is an infinite set, since the constants k_i (cf. equation (4.3)) can have arbitrary integer values. However, from the physical point of view, two angles are indistinguishable if their difference is a multiple of 2π. In the case of finite λ, the distance y could serve as a distinction between two nodes

whose angles differ by $2k\pi$; however, in the limit set $\mathcal{C}_N$, belonging to $\lambda = \infty$, we have $y_i = 0$ identically. Multiples of 2π could be also 'recognized' by the stored energy, however, the $\lambda \to \infty$ limit can be interpreted by letting the flexural rigidity $EI \to 0$, so the energy difference in the links also disappears in the limit. This means, that from the physical point of view we have to take all solutions in $\mathcal{C}_N$ modulo 2π. The resulting set $\mathcal{B}_N$ is defined by

$$\mathcal{B}_N = \{b_i\pi\}; \quad b_i \in \{0,1\}; \quad i \in \{0,1,\ldots,N-1\}. \tag{5.1}$$

where the binary integers b_i can be determined from the corresponding elements of $\mathcal{C}_N$ as

$$b_i = |k_i| \bmod 2.$$

$\mathcal{B}_N$ is (as opposed to $\mathcal{C}_N$) finite, in fact, it is equivalent to the set of all binary strings of length N, so it has exactly 2^N elements. To each element of $\mathcal{B}_N$ an infinite set of elements in $\mathcal{C}_N$ belong. We can regard the elements of $\mathcal{B}_N$ as infinite classes in $\mathcal{C}_N$. Similarly to the labels C_N we define the *binary labels* $B_N = \{b_i\}$ which will prove to be useful when organising the rather complex bifurcational structure of the BVP (4.1)–(4.2). Although the number of distinct binary labels grows rapidly with N, it is still a fixed *finite* number for *all* values of λ, as opposed to the number of branches (and the unique C_N-labels), which grow to infinity. Each physically distinguishable limit solution of the N-link discrete BVP is uniquely characterized by a binary label B_N (cf. the upper part of figure 8: here all physically relevant 16 limit solutions of the four-link BVP are characterized by 2^4 labels.)

(*b*) *The mechanics of Markov chains*

One of the most attractive points of this study is that some of the seemingly abstract limit sets have a direct mechanical analogue. This is perhaps most easily understood in the case of $\mathcal{B}_N$ that can be viewed as the solution set of a *chain* consisting of rigid elements, coupled by frictionless hinges with zero flexural rigidity. The chain is subjected to a single axial end load. In sharp contrast to the discrete elastic structure, the shape of the chain as an IVP cannot be described by a recursion formula; at each node a binary ambiguity enters. (Each element can be either in tension or in compression, *independently* of the previous one.) In other words: the shape of the chain (as an IVP) is *not* determined uniquely by the initial conditions; rather, it can be viewed as a (binary) random walk, perhaps the simplest case of a discrete Markov process, also called (independently from the present application!) a Markov-chain.

As mentioned earlier, Domokos & Holmes (1993*a*) we showed that the recursion formula for the elastic linkage is (under a linear transformation) identical with the standard map, which is known to exhibit chaotic solutions. The chaotic dynamics of the standard map lie at the core of the complex bifurcation diagrams for the BVP (cf. figure 5). We can regard the abundant appearance of parasitic solutions as a manifestation of (spatial) chaotic behaviour in the BVP. The characteristic of this behaviour is that, although deterministic (described by the recursion (4.1)), it exhibits random-like properties. The latter ones can be rigorously formulated only for infinite trajectories (IVPs); however, their presence is also apparent in the finite domain (BVP) as we look at figure 5. Our present study showed that the limit of this behaviour is a random process. Consequently, chaotic dynamics can be either viewed as an infinitely complex, deterministic system, or, equivalently, *as the imperfect (perturbed) version of a random process*. In our case the bending stiffness EI

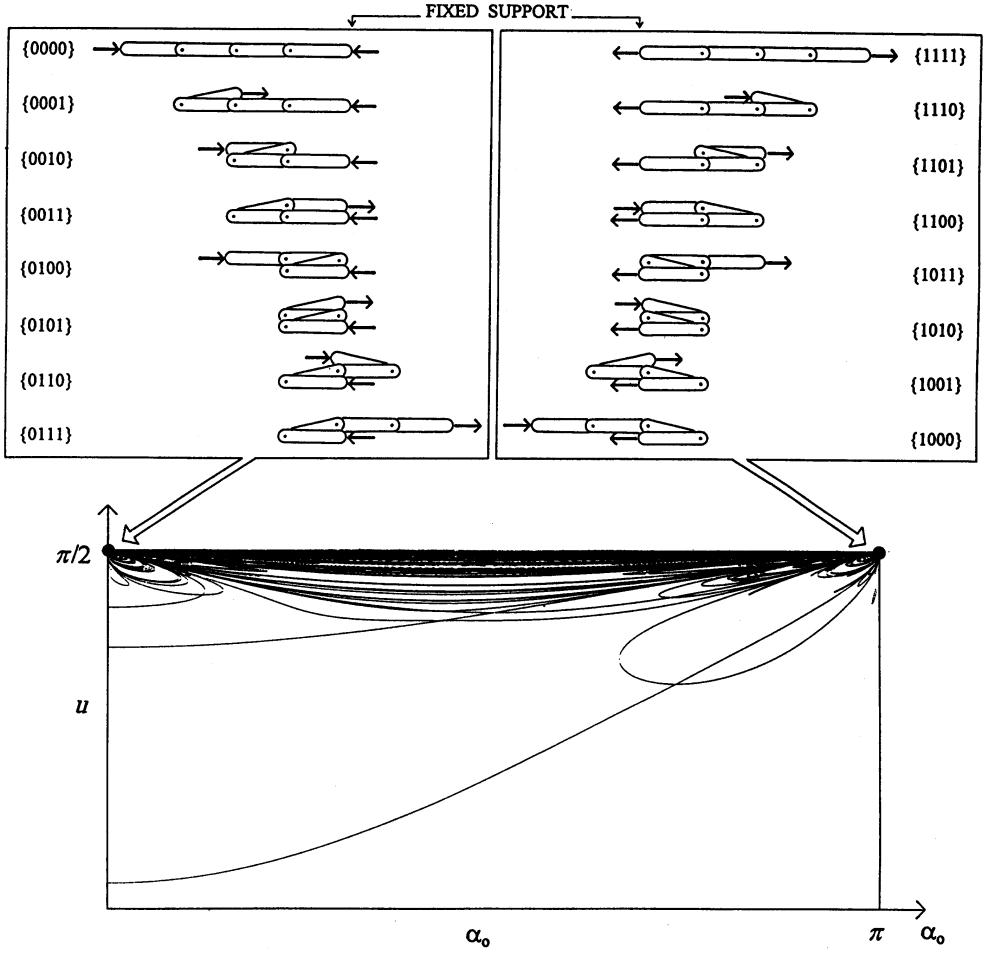

Figure 8. The limit behaviour of the $N = 4$ linkage: 2^4 binary chains.

could serve as a perturbation parameter and we were in the very fortunate situation to demonstrate this random limit as a mechanically meaningful system (chain). Similar (degenerate) random processes might be at the core of other chaotic systems; however, they might not have a direct mechanical interpretation. The appeal of this approach is that the apparently complex behaviour shown in figure 5 boils down to a startlingly simple process. This can be visualized by a rescaling of the parameter λ, bringing $\lambda = \infty$ into the finite range: we let $\lambda = \tan(u)$ ($P = \sin(u)$, $EI = \cos(u)$) and plot the $[\alpha_0, u]$ diagram: as $u \to \frac{1}{2}\pi$ we have $\lambda \to \infty$. Such a diagram for $N = 4$ is illustrated in figure 8, supplemented with the physical shape of the $2^4 = 16$ limit configurations. As mentioned before, uniqueness is violated in the $\lambda \to \infty$ limit, so 8 of the binary chains correspond to $(\alpha_0, u) = (0, \frac{1}{2}\pi)$, and other 8 to $(\alpha_0, u) = (\pi, \frac{1}{2}\pi)$. This result supplements nicely the findings of Domokos & Holmes (1993*a*). The latter referred only to the limit behaviour of the primary branches and claimed that $\alpha_0 \to 0$ or $\alpha_0 \to \pi$ as $\lambda \to \infty$, which is in perfect accordance with the concept of binary chains. Our present study shows that *not only* the primary branches (but all branches) and not only the first angle (but all angles) converge to 0 or π.

(c) *Cardinal numbers and Brouwer's point of view*

The construction of the limit in observation 4.2 could be mapped onto the *mechanical* construction of frictionless chains with decreasing link-size. This intuitive argument guarantees that the limit obtained by our construction falls within the frame of *intuitionistic mathematics*, pioneered by Poincaré and Brouwer. According to the latter, the continuum can be regarded only as a whole ('matrix'), and *not* as an assembly of individual elements (cf. Brouwer 1975).

As observed in § 3, the set $\mathcal{C}$ has the cardinal $\aleph_2$, which is even greater than the cardinal $\aleph_1$ of the continuum. Thus, $\mathcal{C}$ can never be reached directly in any limit starting from a finite set. The limit that we constructed is only a denumerably infinite set $\mathcal{C}^* \subset \mathcal{C}$ with cardinal $\aleph_0$, and could be regarded as the intuitive (or, intuitionistic) version of $\mathcal{C}$. One would expect $\mathcal{C}^*$ to be dense in $\mathcal{C}$, however, this is not the case. It is an interesting question from the engineer's point of view, in which sense $\mathcal{C}$ is approximated by $\mathcal{C}^*$. Similarly, since $\mathcal{W}$ has the cardinal of the continuum ($\aleph_1$), it can not be reached in any intuitive limit (starting from a finite set), only a denumerably infinite, subset $\mathcal{W}^*$. In this case the density does not present difficulty. Neither of these problems arise in the case of $\mathcal{H}$, which is by its definition, (2.5)–(2.6), denumerably infinite.

We did not introduce these considerations earlier since they do not affect the essence of our plausibility argument. The ordering $\mathcal{H} \subset \mathcal{W} \subset \mathcal{C}$ applies also for the constructed (denumerable) limits: $\mathcal{H} \subset \mathcal{W}^* \subset \mathcal{C}^*$. These set-theoretical problems related to mechanical discretization became apparent in our approach because the degree N of discretization appeared in the cardinal number of the solution sets. Otherwise, if the number of solutions does not depend on the discretization, the gap in the cardinal numbers between the approximated set (continuum) and the limit of approximation (denumerable), although still present, is less disturbing. The problems discussed here originate in the choice of the continuum as a convenient mechanical model. It serves this purpose well as long as it is not regarded as a set consisting of individual elements. This approach is not only rejected by the intuitionists, it is also alien to mechanics, a discipline based largely on intuition.

(d) *Stability and the odd-even paradox*

The idea of the inelastic chains casts some light onto the stability of the large number of parasitic solutions appearing in figure 5. It is a natural question to ask whether any, or how many, of these solutions are physically relevant, i.e. stable? The individual study of the solutions is out of question, however, in § 5 *a* we assigned binary labels to each solution. These labels describe the shape of the inelastic chain to which the solution converges. Without detailed argument, appealing to simple experimental intuition, we claim that such a chain cannot be in stable equilibrium if any of the links are compressed. On the other hand, if all elements are in tension, the chain is stable. This means that, at least in the $\lambda \to \infty$ limit, solutions with binary label $B_N = \{b_1, b_2, \ldots, b_N\} = \{1, 1, \ldots, 1\}$ become stable. Although this applies to only *one* of the 2^N binary classes, a single class contains infinitely many solutions.

These considerations lead further, to the (partial) answer to an old-standing paradox about the nth primary mode of the N-link discrete model: as already reported by Gáspár & Domokos (1989): secondary pitchfork bifurcations from the $N-1$ primary branches can be *always* observed if N/n is an even integer, on the other hand, *never* observed if N/n is an odd integer. In the case when N/n is not an integer, no specific conjecture was formulated (cf. figure 5: on lowest branch $N/n = \frac{12}{1} = 12$, secondary pitchfork clearly visible, on fourth mode branch $N/n = \frac{12}{4} = 3$, no secondary

pitchfork can be observed). The question could be generalized in the following form: determine the number b of secondary bifurcations on the nth primary branch of the N-link model. We can not deliver a complete answer; the question still remains open, the complete solution might require deeper tools than ones applied in this paper.

On the other hand, using the concept of binary chains we can determine the *minimal* value $b_{\min}$.

Observation 5.1. *The minimal number $b_{\min}$ of secondary bifurcation on the nth primary branch of the N-link model, can be expressed as $b_{\min} = Nf(n/N)$, where*

$$f(t) = \begin{cases} (1/q), & \text{if } t = (p/q),\ p, q \text{ are relative primes and } q \text{ is even.} \\ 0, & \text{otherwise.} \end{cases}$$

Simultaneously we formulate the following.

Conjecture 5.2. *$b = b_{\min}$ for all (N, n).*

Argument for observation 5.1. In the continuous problem (2.2)–(2.3), as the nth primary branch bifurcates off the trivial solution, the configuration has $E = n - 1$ negative eigenvalues, as it can be shown by linear stability analysis. Maddocks (1984) showed that as $x(L) = 0$, the beam can perform rigid body rotations around $(x, y) = (0, 0)$, corresponding to an unstable bifurcation, the secondary branches of which *do not lie in the α_0, λ plane*. (This is the reason why they do not appear in figure 2: on these secondary branches the vertical force $V(0)$ (cf. figure 1) does not vanish.) This means that, as we pass this bifurcation point in each mode, the number E of negative eigenvalues is increased by one. Since no further bifurcation occurs, in the continuous model the nth primary branch has $E = n$ negative eigenvalues as $\lambda \to \infty$.

The initial count for the negative eigenvalues is identical in the discrete problem (4.1)–(4.2), including the bifurcation at $x_N = 0$ (cf. Domokos & Holmes 1993*a*), so we have $E = n$ on the nth primary branch. However, the $\lambda \to \infty$ limit is rather different. As we saw in § 5 *a*, each branch (including the primary ones) can be characterized by a binary label B_N of length N. The '0' characters correspond to *compressed* chain elements, the '1' characters to the ones in *tension*. The number, E, of negative eigenvalues on any branch in the $\lambda \to \infty$ limit is equal to the number of '0' characters in the corresponding binary string. Let us regard the first mode branch ($n = 1$) of the structures with $N = 4$ and $N = 5$ links, respectively. Contemplation of figure 9 reveals that the $B_4 = \{1111\}$, while $B_5 = \{11011\}$. This means that in the $\lambda \to \infty$ limit we have $E_4 = 0$, $E_5 = 1$.

However, as we discussed before, *initially* we had $E_4 = E_5 = 1$. From the monotonicity of the primary branches (Domokos & Holmes 1993*a*) it follows that limit points do not occur, the only kind of critical point that can change E_4 is a *a secondary bifurcation* (cf. figure 8). The same cannot be claimed for the $N = 5$ case; here E_5 is the same in the limit. (We remark that this does not imply that E_5 remains constant along the branch, however, we did not discover any *necessary* reason for E_5 to change. Conjecture 5.2 claims that the discovered necessary condition is simultaneously a sufficient one.)

The generalization of this observation to the nth primary branch of the N-link structure is purely geometrical. At the bifurcation point from the trivial equilibrium, the nth primary branch consists of n segments of length N/n, separated by intersection points with the load line (not necessarily at joints), displaying n extrema in y.

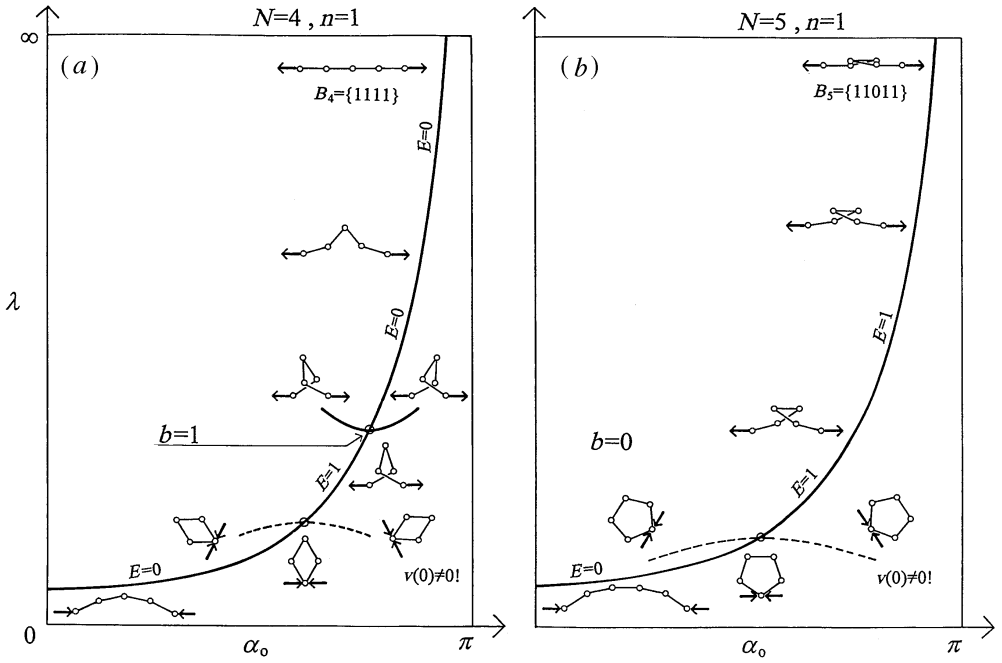

Figure 9. Global behaviour of the $n = 1$ branch for $N = 4$ and $N = 5$.

We have to count, how many *midpoints* of these segments coincide with hinges: those segments will behave similarly to the $N = 4$ branch in figure 8; thus their number is identical to the minimal change in E_N as we move along the branch. As observed before, this number is equal to $b_{\min}$. This geometric count is formulated algebraically in observation 5.1 with the aid of the function $f(t)$. (cf. figure 5: $12 * f(\frac{1}{12}) = 1$; $12 * f(\frac{2}{12}) = 2$; $12 * f(\frac{3}{12}) = 3$; $12 * f(\frac{4}{12}) = 0$; $12 * f(\frac{5}{12}) = 1$; $12 * f(\frac{6}{12}) = 6$; etc.)

We remark that (as it follows from the argument) the number b refers to secondary bifurcation in the $[\alpha_0, \lambda]$ plane and does not include the rigid body rotation at $x_N = 0$.

It seems worthwhile to describe this problem from the point of view of symmetry and symmetry breaking (cf. Golubitsky & Schaeffer 1988). The original problem (both discrete and continuous) has D_2 symmetry in the physical $[xy]$ configuration space. At the *primary* pitchforks the D_2 is factored by one of its subgroups: at *odd* modes by the C_2 (rotation), at *even* modes by the Z_2 (reflection) subgroup. As a consequence, the odd primary branches have Z_2 symmetry, the even primary branches have C_2 symmetry. (For more detail see Domokos & Holmes 1993*a*). In this subsection we dealt only with the first primary mode, so this has Z_2 symmetry, *regardless* of whether N is odd or even. Nevertheless, the $N = 2k$ (even) cases exhibit secondary pitchforks whereas the $N = 2k + 1$ (odd) cases never do so.

At this point it might appear that the reflection symmetry has little to do with the difference between odd and even discretization. This is not the case; Gáspár & Domokos (1989) investigate the behaviour of *symmetrical models*, i.e. non-uniform discretizations that share the symmetry group of the continuous model. (The results of the present paper are generalized for non-uniform discretizations in § 4 *a*.) For the first mode such discretizations are defined by $l_i = l_{N-i+1}$. Gáspár & Domokos (1989) point out that symmetric discretizations consist *typically* of odd number of links; 'even' models are non-generic. Symmetric discretizations are helpful in understanding the transition from 'even' to 'odd' models of uniform discretization. Figure 10

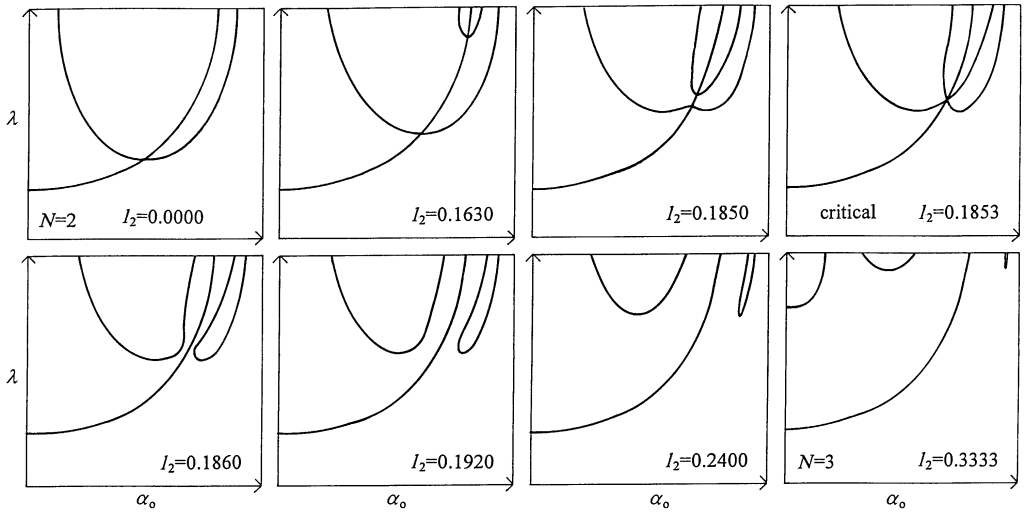

Figure 10. Bifurcation diagrams for the symmetric three-link model.

illustrates eight bifurcation diagrams from the one-parameter family of three-link symmetrical discretizations. The first and last diagram correspond to the $N = 2$ and $N = 3$ uniform discretizations, respectively. The bifurcation behaviour and stability of this structure is described by Maddocks (1985) with analytical tools. The diagrams of figure 10 are in accordance with his results, although he used different parametrization for the links.

(*e*) *Concluding remarks*

In this paper we studied special limits of Euler's buckling problem and of its discretized version. The appearance of imperfect wave-like solutions in physical and numerical experiments motivated our first conjecture, stating that the static image of solitary waves can be obtained by an appropriately constructed limit of the discretized problem. These quasi-static waves are solutions of BVPs that admit the homoclinic loop at arbitrary locations. We supported our conjecture by a plausible argument: we proved that a larger and a smaller set can be equally reached as limits.

These limits sets proved to be very helpful in organising the complex bifurcational structure of the discrete problem. In particular, we were able to assign individual unique labels to all branches in the N-link problem in the form of integer strings of length N. These labels open many interesting questions, e.g. they could be the basis of accurate estimates on the number of parasitic solutions. Branches can be ordered according to the parameter values where they emerge, or, according to their labels. The relationship between these orderings seems to be a challenging problem. We also defined binary labels, characterizing the stability at infinity. With the aid of these labels we were able to answer an old question: why does the behaviour of models with even and odd N differ? The construction of binary labels leads to the observation that the limit of this spatially complex behaviour is an appealingly simple random walk, or, conversely, spatial chaos in this BVP can be viewed as a perturbation of a Markov process. We hope that beyond making our conjecture on wave-like solutions plausible, the study of this simple mechanical example contributes to the better understanding of the relationship between discrete and continuous structures, their limits, and to the concepts relating chaotic and random behaviour.

The author highly appreciates the stimulating discussions with László Fehér, Zsolt Gáspár and Phil Holmes. The support of OTKA grants no. F021307 and no. T015851 is gratefully acknowledged. The fast and precise preparation of the figures is due to Antónia Szabados.

References

Beyn, W.-J. 1982 Spurious solutions for discrete superlinear boundary value problems. *Computing* **28**, 43–51.

Beyn, W.-J. 1990 The numerical computation of connecting orbits in dynamical systems. *J. Num. Analysis* **9**, 379–405.

Bohl, E. 1979 On the bifurcation diagram of discrete analogues for ordinary bifurcation problems. *Math. Meth. Appl. Sci.* **1**, 566–571.

Brouwer, L. E. J. 1975 *Collected works* (ed. A. Heyting), vol. I, pp. 82–83, 102–104. Amsterdam: North Holland.

Coleman, B. D. & Dill, E. H. 1992 Flexure waves in elastic rods. *J. Acoust. Soc. Am.* **91**, 2663–2673.

Domokos, G. & Holmes, P. J. 1993*a* Euler's problem, Euler's method and the standard map. *J. Nonlinear Sci.* **3**, 109–151.

Domokos, G. & Holmes, P. J. 1993*b* On non-inflexional solutions of non-uniform elasticae. *Int. J. Nonlin. Mech.* **28**, 677–685.

ElNaschie, M. S. 1990 On the suspectibility of local elastic buckling to chaos. *ZAMM* **70**, 535–542.

Euler, L. 1744 *Methodus inveniendi lineas curvas maximi minimive proprietate gaudentes Ostwald's Klassiker der Exakten Wiss.* vol. 75. Leipzig: W. Engelmann. (In German.)

Fraenkel, A. 1923 *Einleitung in die Mengenlehre.* (Grundl. der Math. Wiss., vol. IX). Berlin: Springer.

Gáspár, Zs. & Domokos, G. 1989 Global investigation of discrete models of the euler buckling problem. *Acta Technica Acad. Sci. Hung.* **102**, 227–238.

Golubitsky, M. & Schaeffer, D. 1988 *Singularities and groups in bifurcation theory*, vol. I, vol. II (with I. Stewart). Berlin: Springer.

Kirchhoff, G. 1859 Über das Gleichgewicht und die Bewegung eines unendlich dünnen elastischen Stabes. *J. für Math. (Crelle)* **56**, 285–313.

Love, A. E. H. 1927 *A treatise on the mathematical theory of elasticity* New York: Dover.

Maddocks, J. H. 1984 Stability of nonlinearly elastic rods. *Arch. Ration. Mech. Analysis* **85**, 311–354.

Maddocks, J. H. 1985 Restricted quadratic forms and their application to bifurcation and stability in constrained variational principles. *SIAM J. Math. Analysis* **16**, 47–68.

Maddocks, J. H. & Dichmann, D. J. 1994 Conservation laws in the dynamics of rods. *J. Elasticity* **34**, 83–96.

Marsden, J. E., O'Reilly, O., Wicklin, F. J. & Zombro, B. W. 1991 Symmetry, stability, geometric phases and mechanical integrators. *Nonlinear Sci. Today* **1** 4–11, 14–21.

Mielke, A. & Holmes, P. 1988 Spatially complex equilibria of buckled rods. *Arch. Ration. Mech. Analysis* **101**, 319–348.

Peitgen, H.-O. & Schmitt, K. 1981 Positive and spurious solutions of nonlinear eigenvalue problems. In *Numerical solution of nonlinear equations* (ed. E. L. Allgower, K. Glashoff & H.-O. Peitgen). Springer Lecture Notes in Mathematics, no. 878, pp. 276–324.

Peitgen, H.-O., Saupe, D. & Schmitt, K. 1981 Nonlinear elliptic boundary value problems versus their finite difference approximations: numerically irrelevant solutions. *J. Reine U. Angew. Math. (Crelle)* **322**, 74–117.

Polya, G. 1968 *Mathematics and plausible reasoning*, 2nd edn. Princeton University Press.

Thompson, J. M. T. & Virgin, L. N. 1988 Spatial chaos and localization phenomena. *Phys. Lett.* A **126**, 491–496.

Walsh, J. L. 1923 A closed set of normal orthogonal functions. *Am. J. Math.* **45**, 5–24.